RSC Advances

PAPER

View Article Online
View Journal | View Issue

Cite this: *RSC Adv.*, 2015, **5**, 16727

An Au–Cu bimetal catalyst for acetylene hydrochlorination with renewable γ-Al_2O_3 as the support†

Jigang Zhao,*[a] Junjian Zeng,[a] Xiaoguang Cheng,[a] Lei Wang,[ab] Henghua Yang[a] and Benxian Shen[a]

Received 2nd November 2014
Accepted 21st January 2015

DOI: 10.1039/c4ra13648a

www.rsc.org/advances

The bimetal catalyst gold(III) chloride–copper(II) chloride ($AuCl_3$–$CuCl_2$) was prepared with several different gamma-aluminium oxide (γ-Al_2O_3) supports and its catalytic properties towards acetylene hydrochlorination were assessed in a fixed-bed reactor. The comparison indicated that one of the catalysts attained the highest activity with an acetylene conversion of 97%, which was far higher than the others. Catalysts were characterized using detailed X-ray diffraction, nitrogen-Brunauer, Emmett and Teller surface area analysis (N_2-BET), ammonia temperature-programmed desorption, Fourier-transform infrared spectroscopy and carbon dioxide temperature-programmed desorption analysis. It is proposed that the base site contributed to its high catalyst activity compared with the other catalysts, instead of the acid site or the textural properties on the support, therefore, the activity and the life of the catalysts can be improved significantly by treating the supports with potassium hydroxide. In addition, the results of N_2-BET, thermogravimetric analysis and scanning electron microscopy indicated that the catalysts deactivated rapidly because of carbon deposition, and the actual amount of coke deposition was 18.0% after the reaction. $AuCl_3$–$CuCl_2$/γ-Al_2O_3 was easily regenerated for reuse as a catalyst by burning off in an air atmosphere for 10 min. The activity of the regenerated catalyst nearly reached the level of the fresh catalyst.

1. Introduction

Vinyl chloride monomer (VCM) is mainly used for the synthesis of poly(vinyl chloride), which is widely used in every aspect of life.[1] In China, about 70% of the VCM products are produced from acetylene hydrochlorination, which is based on the catalyst mercury(II) chloride ($HgCl_2$) supported on activated carbon (AC).[2,3] However, the toxicity and volatility of $HgCl_2$ can cause serious trouble to the environment and human health, which has driven many researchers to study non-mercuric catalytic systems. Nowadays, gold (Au) is regarded as an efficient catalyst metal.[4,5] Conte *et al.*[6,7] studied the AU catalyst in detail and found that Au has high activity in the acetylene hydrochlorination reaction. Its initial activity was higher than that for the $HgCl_2$ catalyst. Alloying Au with other base metals is a promising way to improve the catalytic activity and a bimetallic gold–copper (Au–Cu)/AC catalyst showed promising catalytic activity and an acetylene conversion of 99.5% at 200 h.[8] Au-based catalysts have drawn many researchers' attention, however, most of them were focused on AC as the support which has low mechanical strength and poor regeneration capacity.[9] In normal practice, the Au dosage was more than 1% of the carbon support, which makes the catalyst too expensive for large scale use. This prompted us to consider whether there was a better support for using acetylene hydrochlorination rather than the AC. According to reports, Au-based catalysts have very low activity when using titanium dioxide or silicon dioxide as the support.[10]

In our previous work, it has been demonstrated that the bimetal Au–Cu catalyst has superior activity and longer lifetimes compared with the industrially preferred catalyst, which is based on carbon supported $HgCl_2$.[8] Efforts have also been undertaken to explore aluminium oxide (Al_2O_3) as a non-mercury catalyst support to reduce the Au content for acetylene hydrochlorination.[11] In addition, it was found that for the oxygen-containing groups, especially for the hydroxyl groups, the AC played an important role in the high activity and excellent stability of the Au–Cu/AC catalyst.[13] Because of the lack of mesopores and macropores in the carbon, the chloroauric acid ($HAuCl_4$) solution with 40–200 nm gold(III) chloride ($AuCl_3$) particles[12] cannot diffuse into the inner part effectively, which will inevitably lead to aggregation of the $AuCl_3$ particles on the surface and also in the outer shell of the AC pellets. The fact that

[a]*State Key Laboratory of Chemical Engineering, East China University of Science and Technology, 130 Meilong Road, Shanghai 200237, P. R. China. E-mail: zjg@ecust.edu.cn; Fax: +86 21 64252851; Tel: +86 21 64252916*

[b]*TianjinDagu Chemical Co., Ltd., 1 Xinghua Road, Tianjin 300455, P. R. China*

† Electronic supplementary information (ESI) available. See DOI: 10.1039/c4ra13648a

Au^{3+} was absorbed on the mesopores of the AC shows that this is the main site of activity while the micropores can be ignored in order to improve the usage of Au.[12] Meanwhile, the discontinuous distribution and disposable activity were its major shortcomings. All the above facts prompted us to consider whether gamma-aluminium oxide (γ-Al_2O_3), which has a mesoporous (20–50 nm) structure and contains abundant hydroxyl groups on the surface, could be an efficient support for Au-based catalysts in acetylene hydrochlorination. Recently, γ-Al_2O_3 was used as the support for preparing Au-based catalysts for carbon monoxide oxidation[14,15] and hydrodechlorination of carbon tetrachloride.[16] However, as far as we are concerned, there is very little literature[11,12] reporting Au-based catalysts supported on γ-Al_2O_3, and there is still much room for improvement.

In this work, the γ-Al_2O_3 was employed as the support for the gold(III) chloride–copper(II) chloride ($AuCl_3$–$CuCl_2$) catalyst for acetylene hydrochlorination. Because of its mesoporous structure, $AuCl_3$–$CuCl_2$ supported on γ-Al_2O_3 can effectively reduce the content of the Au component. It was found that some γ-Al_2O_3 have some special characteristics, and that they can be efficient supports for the catalyst. The possible mechanisms accounting for the enhanced stability and catalytic efficiency are also discussed. The effects of textural properties and acid/base site of the γ-Al_2O_3 support on the catalyst activity were also studied in detail. In addition, the reasons for deactivation and the regeneration method were also investigated.

2. Experimental section

2.1 Catalyst preparation

Bimetallic Au–Cu/γ-Al_2O_3 catalysts were prepared using an incipient wetness impregnation technique.[8] γ-Al_2O_3 (A, B, C, D) from different companies (10 g, Hengxin, Yuanheng, Hong Xing and BaoLai Co. Ltd, China) were initially washed with dilute aqueous hydrochloric acid (HCl; 1 mol l^{-1}) at 25 °C for 1 h to remove the impurities on the surface. Then the catalyst was prepared by impregnating the γ-Al_2O_3 with 2 ml of $HAuCl_4 \cdot 4H_2O$ (Au content assay 49.7%) *aqua regia* solution (1 g $HAuCl_4 \cdot 4H_2O$/100 ml) and 20 ml of $CuCl_2 \cdot 2H_2O$ solution (6.25 g $CuCl_2 \cdot 2H_2O$/500 ml), stirred for 3 h at 353 K, then dried at 423 K for 12 h. The catalysts prepared by different supports were donated as ACAlA, ACAlB, ACAlC, ACAlD. Some of the catalysts were named MAC-AlB, namely B pretreated with potassium hydroxide (KOH) denoted as MB, and the catalysts were prepared based on the process described elsewhere,[8] in order to distinguish the effect of basic sites.

2.2 Catalyst characterization

Brunauer, Emmett and Teller (BET) surface area analysis and pore size distribution were performed by obtaining nitrogen (N_2) adsorption isotherms at 77 K using a ASAP2020 accelerated surface area and porosimetry analyzer (Micromeritics). Temperature programmed analysis including carbon dioxide temperature-programmed desorption (CO_2-TPD) and ammonia temperature-programmed desorption (NH_3-TPD) was performed using the ASAP 2920, using 10% CO_2 (or NH_3) in argon (flow 50 ml min^{-1}, holding for 30 min) as the adsorption gas and a temperature ramp from 50 to 700 °C (ramp rate, 10 °C min^{-1}) when adsorbing. The morphology of the samples was examined using scanning electron microscopy (SEM) with a Nova NanoSEM 450 (FEI, The Netherlands). X-ray diffraction (XRD) data were collected using a D8 advanced X-ray diffractometer (Bruker) with Cu-Kα irradiation at 40 kV and 40 mA in the scanning range from 10° to 80°. Hydrogen temperature-programmed desorption (H_2-TPR) was performed using the ASAP 2920, using 10% H_2 in argon (flow 50 ml min^{-1}) as the reductive gas and a temperature ramp of 50 to 600 °C (ramp rate, 10 °C min^{-1}) with a thermal conductivity detector recording the signal. Fourier-transform infrared (FT-IR) spectra were obtained using a 6700 FT-IR spectrometer (Thermo Fisher Nicolet). XPS data were collected using an Axis Ultra spectrometer (Kratos Analytical) with a monochromatized Al-Kα X-ray source and a minimum energy resolution of 0.48 eV (Ag $3d_{5/2}$).

2.3 Catalyst testing

The catalytic performance for acetylene hydrochlorination was evaluated in a fixed-bed microreactor (diameter 10 mm) operating at a pressure of 0.1 MPa and a temperature of 150 °C. The reactor was purged with N_2 to remove water in the reaction system before the reaction occurred. Hydrogen chloride passed through the reactor at a flow rate of 50 ml min^{-1} for 2 h to activate the catalyst. After the reactor was heated to 150 °C, acetylene (20 ml min^{-1}) and hydrogen chloride (22 ml min^{-1}) were fed through the heated reactor, which contained 10 ml of catalyst. The reaction product was analyzed by gas chromatography (GC-920, Al_2O_3 PLOT column). The catalyst activity was determined by the conversion of acetylene ($X_{C_2H_2}$) and selectivity of VCM (S_{VCM}), which are defined as:

$$X_{C_2H_2} = (1 - \Phi_{C_2H_2}) \times 100\% \quad (1)$$

$$S_{VCM} = \Phi_{VCM}/(1 - \Phi_{C_2H_2}) \times 100\% \quad (2)$$

Of which $\Phi_{C_2H_2}$ is the residual volume fraction of acetylene and Φ_{VCM} is the volume fraction of chloroethylene.

3. Results and discussion

3.1 Catalytic activity

Catalysts with different supports were used in a fixed bed reactor to assess their catalytic performance for acetylene hydrochlorination. The $X_{C_2H_2}$ and S_{VCM} with reaction time are illustrated in Fig. 1. It shows that all the catalysts had excellent selectivity toward vinyl chloride (C_2H_3Cl) (Fig. 1a). However, their activities were quite different (Fig. 1b). The catalysts' activity initially exhibited a growing trend, but then decreased after running for 2 h. ACAlD had the best performance among the samples with the highest conversion of 96% and stabilization of about 90%. For comparison, the three other catalysts had conversions from 40% to 80%, which were significantly lower.

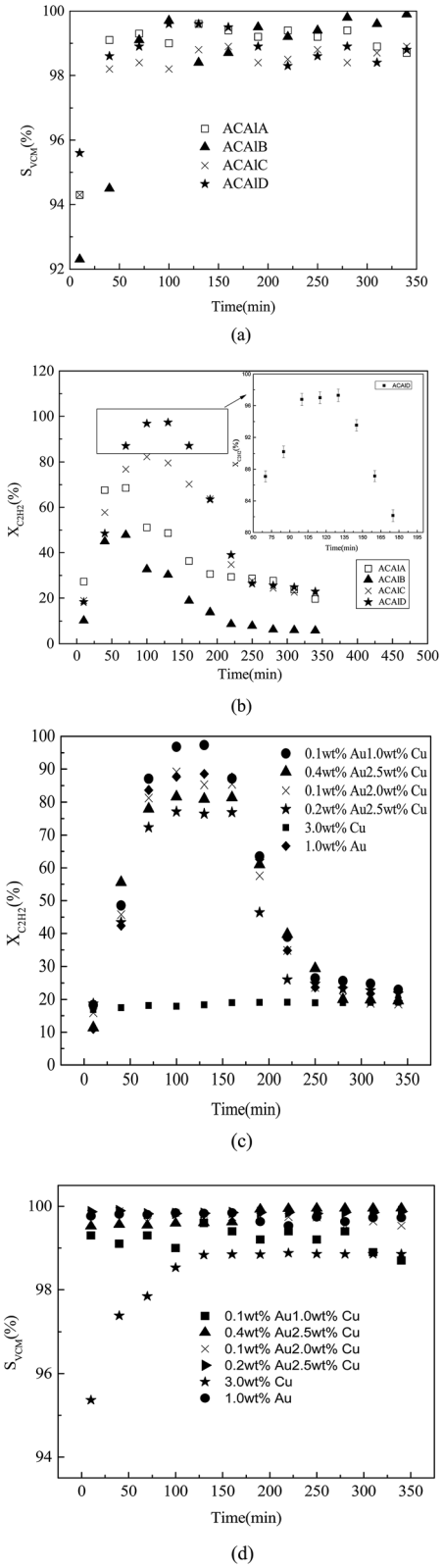

Fig. 1 Various curves of (a) C_2H_3Cl selectivity with time and (b) C_2H_2 conversion with time. (c) Influence of Au^{3+}/Cu^{2+} content on the catalysts for acetylene conversion. (d) Influence of Au^{3+}/Cu^{2+} contents on the catalysts for C_2H_3Cl selectivity. Temperature = 150 °C, pressure = 0.1 MPa, V(HCl) : V(C_2H_2) = 1.1 : 1, gas hourly space velocity (GHSV) = 120 h^{-1}.

The ACAlD had the highest C_2H_2 conversion, which was contrary to its minimum S_{BET} (Table 1). This could not be explained by the traditional viewpoint that the higher the S_{BET}, the better the catalyst activity when using the AC as the support.[14] It can be seen that the volume of porosity per unit volume (V_p) and average pore diameter (D_p) values of sample D were higher than those of the others. However, the corresponding values of sample A were higher than those of sample C, and sample A's catalytic activity was lower than that of sample B. Additionally, samples B and C had almost the same textural parameters, however, they had significantly different catalytic activities. These results demonstrate that the textural parameters of the support were not the main reason for the different catalytic activities. It is the surface chemical properties that play an important role in the catalyst system, and this needs to be studied further, in more detail.

Fig. 1c and d show the influence of the Au^{3+}/Cu^{2+} content on the structured catalysts supported by D on acetylene conversion and C_2H_3Cl selectivity. The amounts of Au loaded on each were 0.1 wt%, 0.4 wt%, 0.1 wt%, 0.2 wt%, 0.1 wt% and 0 wt% on six corresponding D supports, which were coated with 1.0 wt%, 2.5 wt%, 2.0 wt%, 2.5 wt%, 3.0 wt% and 0 wt% Cu, respectively. As can be seen from the Fig. 1c, the catalytic activity improved significantly, when added and improved Au components in the catalysts, as compared with single-component Cu catalysts, which confirmed that $AuCl_3$ plays an important role in the catalytic performance. Nevertheless, it was found that when both the Au and Cu were added in certain ratios, as shown, the catalyst could achieve more satisfactory conversion and lower Au dosage compared with single component Au catalysts. This result demonstrates that adding $CuCl_2$ could reduce the amount of precious metal Au required significantly, thus reducing the cost of the catalyst.

3.2 Characterization techniques

3.2.1 XRD characterization and N_2 adsorption/desorption studies. The XRD patterns of the four γ-Al_2O_3 are shown in Fig. S1(ESI†). They indicate that all the supports have a similar crystal structure. The N_2 adsorption desorption isotherms and the pore size distribution of four γ-Al_2O_3 supports are illustrated in Fig. S2a and S2b(ESI†). The textural parameters of the

Table 1 Textural characterization

Sample	S_{BET}[a] (m^2 g^{-1})	V_p[b] (cm^3 g^{-1})	D_p[c] (nm)
A	244.1	0.495	7.60
B	295.0	0.400	6.25
C	310.4	0.406	6.55
D	188.8	0.486	9.34
Fresh ACAlA	245.3	0.496	7.58
Fresh ACAlB	294.1	0.405	6.26
Fresh ACAlC	311.2	0.406	6.53
Fresh ACAlD	186.4	0.493	9.29
Deactivated ACAlD	179.4	0.479	8.89

[a] BET specific surface area. [b] Barret–Joyner–Halenda (BJH) volume of pores. [c] Average pore diameter.

γ-Al_2O_3 are listed in Table 1. BET surface areas (S_{BET}) values were obtained within the range of 188.8–310.4 $m^2\ g^{-1}$. Samples B and C had similar textural parameters, whose S_{BET} values (295.0 $m^2\ g^{-1}$ and 310.4 $m^2\ g^{-1}$) were higher than those of samples A and D (244.1 $m^2\ g^{-1}$ and 188.8 $m^2\ g^{-1}$).

Because the AC surface is very dense, the lack of mesoporous structure[12] means that the $HAuCl_4$ solution cannot enter the inner part of the dense AC pellets. The high density $AuCl_3$ and $CuCl_2$ crystals accumulated on the surface and also in the outer shell of the AC pellets will inevitably aggregate to form large clusters. By contrast, Al_2O_3 is rather porous,[11] leading to good dispersion of the $AuCl_3$ particles, which enhanced the utilization of Au to a certain extent. This result combined with the previously mentioned C_2H_2 conversion results can be prove efficiently that using Al_2O_3 as supports for preparing catalysts can reduce the Au content.

3.2.2 Temperature-programmed analyses. The CO_2-TPD profiles for all the pure γ-Al_2O_3 are shown in Fig. 2a. Compared with samples A, B and C, a medium intensity desorption peak and a strong desorption peak could be observed in the profile of sample D, which indicates that sample D has a medium and a strong base site. In addition, there were considerable differences in the weak base site among the four samples. The shifts in desorption peaks of the weak base site were related to $X_{C_2H_2,max}$; it could be observed that the two values revealed a positively proportional relationship (Fig. 2b), namely the

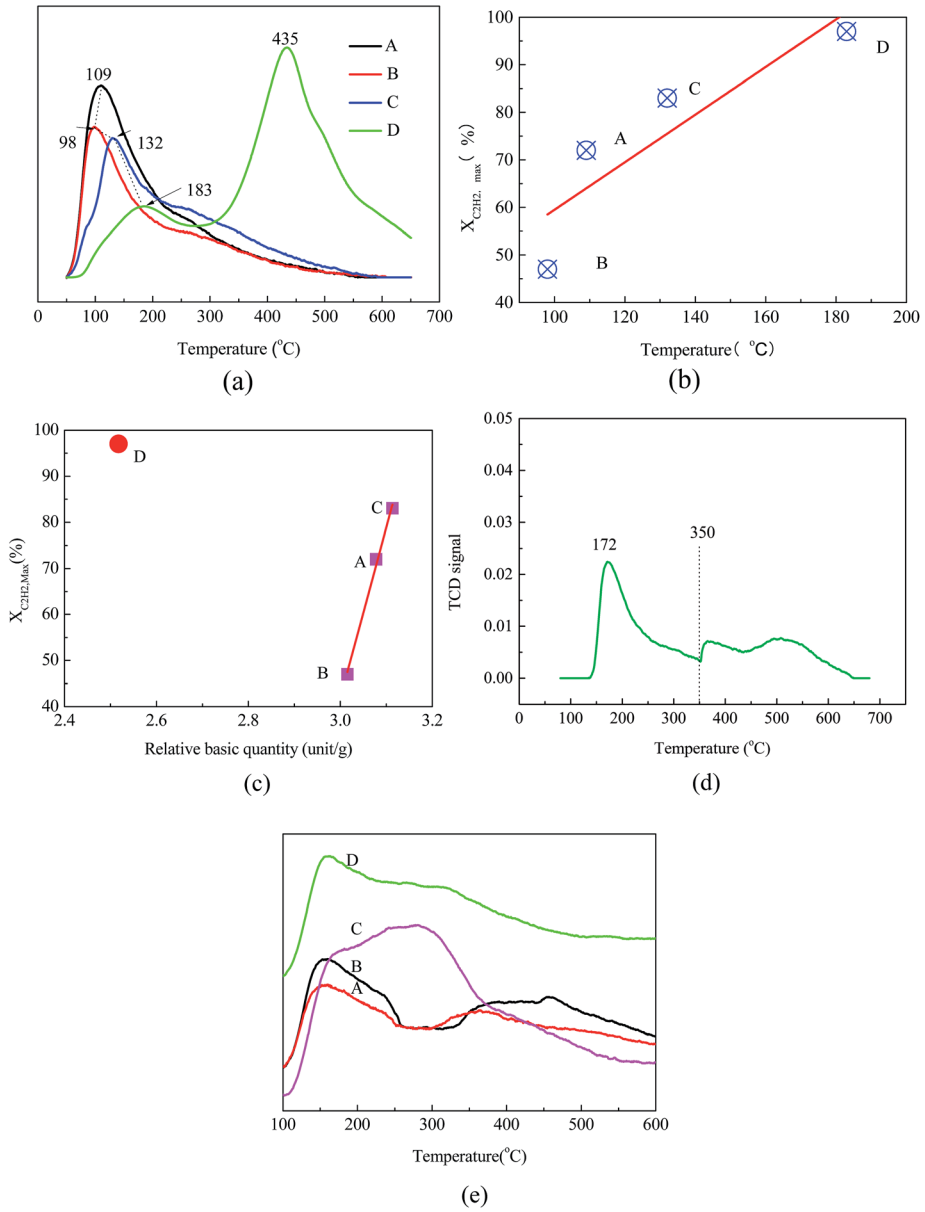

Fig. 2 TPD profiles and their correlation. (a) CO_2-TPD profiles of alumina A, B, C and D. (b) Correlation between catalytic activity and basic strength. (c) Correlation between catalytic activity and relative basic quantity. (d) CO_2-TPD profile of fresh ACAlD. (e) NH_3-TPD profiles of alumina A, B, C and D.

higher the temperature, the higher the $X_{C_2H_2,max}$. That is to say strengthening the weak base site of the γ-Al_2O_3 support could enhance the activity of the $AuCl_3$–$CuCl_2/\gamma$-Al_2O_3 catalyst, and the amount of basic sites (including the medium and strong base sites in sample D) of the four samples is also related to the $X_{C_2H_2,max}$; the profile showed a linear relation (Fig. 2c). Curiously, sample D had the least amount of basic sites, but it had the highest catalytic activity. This could be explained by the excess medium and strong basic sites in sample D. To confirm the above conclusion, a CO_2-TPD experiment was conducted on the fresh ACAlD catalyst and the results are shown in Fig. 2d. It can be clearly seen that the strong basic site on the alumina D is reduced above 350 °C. This may be the reason that there is an interaction effect between Au^{3+} and the strong basic site on the alumina surface when absorbed.

The NH_3-TPD patterns are shown in Fig. 2e. All the samples had a weak acidic site and samples A, B, and D had similar weak acids with a desorption peak of about 150 °C, while the tail of the desorption peak of sample D was shifted to higher temperatures (about 450 °C). In addition, according to the size of the area under the NH_3-TPD profiles, the amount of acidic sites is in the following order: D > C > A > B. Among them, sample C had an obvious feature of medium acidic sites, and a handful of strong acidic sites in sample A and D could be observed. Although some efforts had been made to correlate the C_2H_2 conversion with the acid strength and amount of acidic sites, just as in the previous method of investigation of the basic sites, it showed that there was no clear trend between the acidic properties of the support and the overall rate of C_2H_2 conversion.

The influence of the basic site of the catalysts activity using different γ-Al_2O_3 as the support has been investigated. The H_2-TPR profiles of the fresh ACAlA, ACAlB, ACAlC, and ACAlD are shown in Fig. S3(ESI†) and the transmission electron microscopy images of them are shown in Fig. S4(ESI†). They indicate that the base site on the surface of the γ-Al_2O_3 support has a positive effect on the dispersion of the active ingredient.

3.2.3 X-ray photoelectron spectroscopy (XPS). To further demonstrate the basic sites and determine the oxidation states of the surface Au sites on the catalyst's[17] surface, the XPS spectra of the fresh ACAlD catalyst corresponding to Au 4f peaks and O 1s peak are shown in Fig. 3. Three broad peaks appeared over the Au 4f region, which could be deconvoluted, to components because of gold(III) hydroxide ($Au(OH)_3$) gold(III) oxide (Au_2O_3), and metallic Au. The Au^0 $4f_{7/2}$ peaks were detected at a range of binding energy of 83.0–83.1 eV, which was typical of metallic Au, and the spectra with binding energies at 86.2 and 89.9 eV were attributed to the presence of Au in the form of Au^{3+}.[18] From the binding energy of the O 1s XPS, different basic sites on the catalyst surface could be determined. All of the O (1s) signals, wide and asymmetrical, were deconvoluted into four components responding to diversified O atom species, which indicated the presence of oxygen atoms in four different chemical environments, including OH^- peaks at about 531–532 eV, lattice oxygen complex metal oxides, such as M–O–M, at 530.1 eV, O^{2-} in CuO at 529.6 eV and a relatively strong peak at a lower binding energy of about 528.5 eV, which could be attributed to the low-coordinated $O^{\delta-}$.[19] Based on the two points above, it could be concluded that the catalyst surface contained different chemical groups and by anchoring these chemical groups, active sites could be more effectively loaded on the catalyst surface.

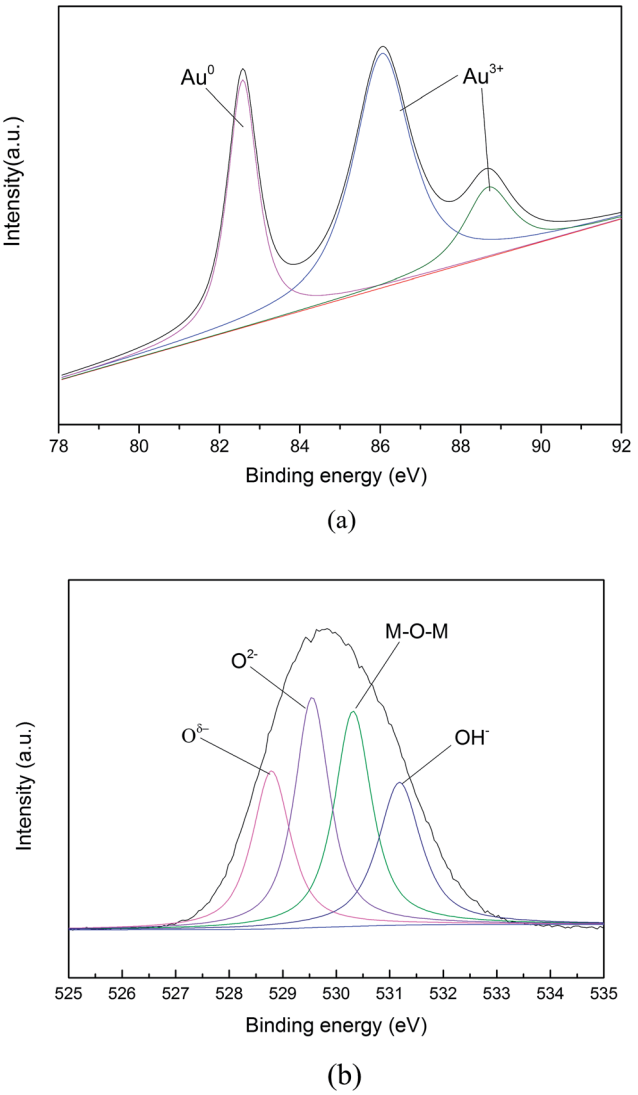

Fig. 3 (a) XPS spectra of Au 4f in fresh ACAlD catalyst. (b) XPS spectra of O 1s spectrum in the fresh ACAlD catalyst.

3.3 Initial support modification using potassium hydroxide

Cornelius[20] reported that support modification using KOH produced O^{2-} or O^-, which can provide a Lewis base site on the surface of Al_2O_3 during the process of dehydration after calcination. It may be that the different oxygen centers of the O^{2-} or O^- on the surface of Al_2O_3 can affect the nucleation process of Au^{3+} and Cu^{2+} species adsorbed on the surface, and this could lead to different particle sizes of active ingredient on different supports (Fig. S5 ESI†), however, the mechanism should be studied further.

To confirm that the surface base sites of the support play an important role in the excellent performance of alumina, alumina B, which had the worst catalytic performance, was

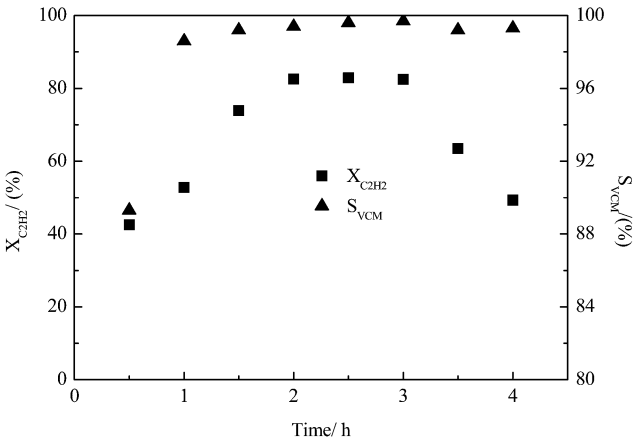

Fig. 4 Curves showing the variation of C_2H_2 conversion and C_2H_3Cl selectivity with time for MACAlB. Temperature = 150 °C, pressure = 0.1 MPa, V(HCl) : V(C_2H_2) = 1.1 : 1, GHSV = 120 h^{-1}.

initially modified by KOH. After being cleaned using HCl, alumina B was impregnated for 10 h in 5 mol l^{-1} KOH solution and then dried. The sample obtained was designated MB. As the previously mentioned steps were done, the MACAlB catalyst was also prepared with MB as the support. The CO_2-TPD profile of MB is shown in Fig. S6(ESI†) and it can be seen that an obvious strong basic site has appeared. Compared with ACAlB, the catalytic performance (Fig. 4) of MACAlB had improved significantly and the highest conversion rate was increased from 51% to 82%. To account for the surface groups of the supports, the FT-IR spectra of different samples (C, B, MB, ACAlB, MACAlB) were analyzed. As can be seen from Fig. 5, the obvious bands were observed at 3497.08 cm^{-1} and 1640 cm^{-1}, which are the hydroxyl absorption peaks of water. Bands at 729.45 cm^{-1} and 566.09 cm^{-1} are regarded as the weak absorption peaks of γ-Al_2O_3. There were two obvious differences in the patterns between the fresh and modified catalysts: characteristic peaks of hydroxyl radicals from Al–OH on the surface of the γ-Al_2O_3 at 1161 cm^{-1} and 1437 cm^{-1} are characteristic absorption peaks of AlO_2^-.[21] It was found that after loading the active metal, the AlO_2^- peaks became weaker, which indicates that the process of loading caused the electron transformation. Therefore, a strong effect of the surface chemistry of modified Al_2O_3 on the Au–Cu/Al_2O_3 catalytic activity was observed, as shown in Fig. 4.

In addition, the life span was also extended, showing that the basic sites on the support play an important role in improving the catalyst activity and its life span.

3.4 Deactivation analysis

The specific surface area and pore structure parameters of both the fresh ACAlD and the deactivated ACAlD catalyst are shown in Table 1. It can be seen that the parameters of the fresh catalyst are similar to those of the support, which suggests that it did not produce the reunion and bridging phenomenon with small particle size $AuCl_3$ and $CuCl_2$ loaded on the mesoporous pore surface of γ-Al_2O_3. There was nearly no change in the channel and specific surface area of the fresh catalyst with the support. However, the parameters of the deactivated catalyst were reduced. It seems that there was a phenomenon of channel jam in the catalyst during the reaction.

SEM images of the fresh and deactivated catalysts are shown in Fig. 6. It can be clearly seen that channels are relatively abundant in the fresh catalyst (Fig. 6a). However, the surface of the deactivated catalyst was covered with a layer of carbon deposition with a "chip" structure (Fig. 6b). The 'chip' structure deposition covered the active sites and was produced quickly and easily and this was one reason for the catalyst's short life

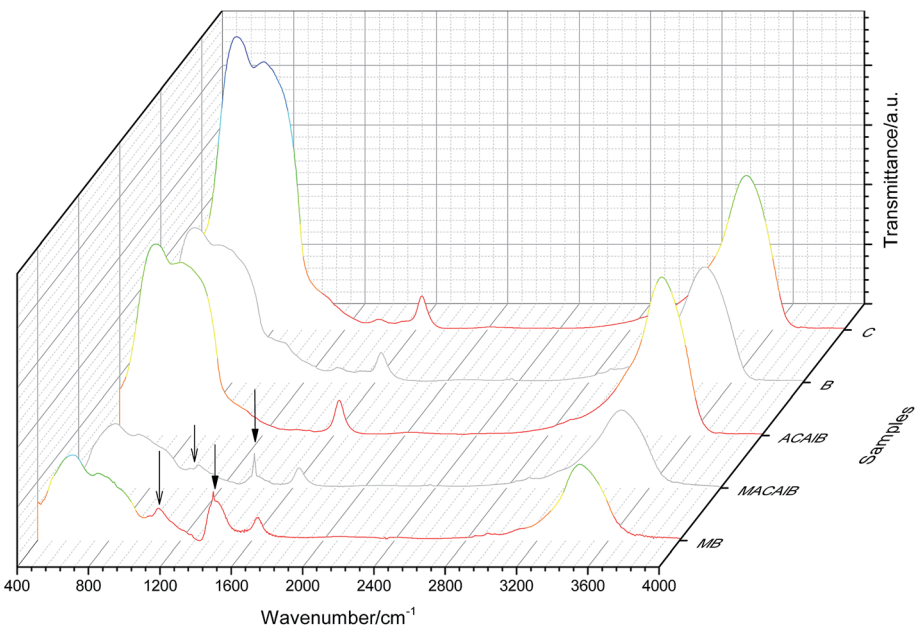

Fig. 5 FT-IR spectra of pure support C, support B, the fresh catalyst ACAlB, the modified catalyst MACAlB and the modified support MB.

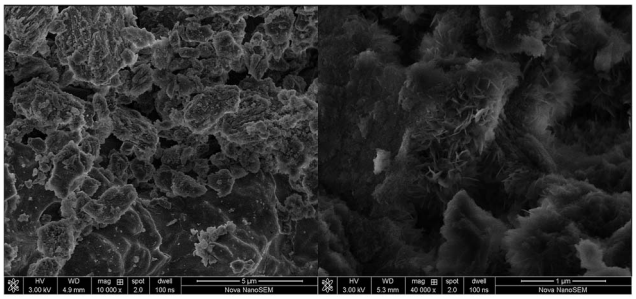

Fig. 6 SEM images of (a) the fresh catalyst and (b) the deactivated catalyst.

span. In addition, this was consistent with the results of the N_2 adsorption and desorption analysis (Table 1).

In order to provide direct evidence of coke deposition, thermogravimetric analysis (TGA) was performed under an air atmosphere and the results are shown in Fig. 7. The amount of coke deposition should be equal to the difference in weight loss between the fresh and deactivated catalysts within the temperature range of coke burning. The mass losses of fresh and deactivated ACAlD catalysts in the range of 100–500 °C were 3.9% and 21.9%, respectively, which indicates that the actual amount of coke deposition was 18.0%. This also demonstrates that the coke deposition could be nearly burned off at a temperature of 500 °C in an air atmosphere.

3.5 Regeneration studies

Because of the high price of Au, the possibility of reusing the catalyst was also investigated (Fig. 8). The deactivated catalyst could be easily regenerated by roasting it at 500 °C in an air atmosphere for 10 min. The process was simple and the high mechanical strength of the γ-Al_2O_3 support guaranteed the intact shape of the catalyst when loading and unloading. It can be seen that the C_2H_2 conversion rate can reach 96% and the C_2H_3Cl selectivity was more than 99% for the first regenerated catalyst, which was nearly the same catalytic performance as the fresh catalyst. However, the activity of the twice regenerated

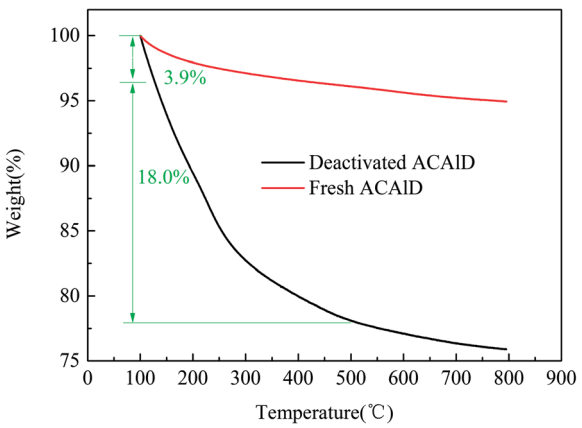

Fig. 7 TGA profiles of fresh ACAlD and deactivated ACAlD.

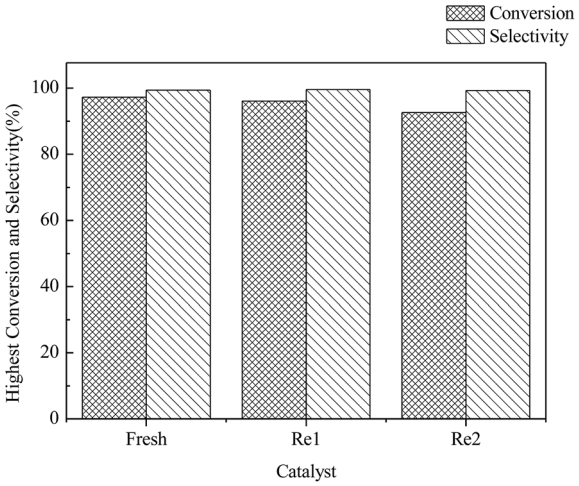

Fig. 8 The highest C_2H_2 conversion and C_2H_3Cl selectivity of the fresh and regenerated catalyst. Temperature = 150 °C, pressure = 0.1 MPa, $V(HCl) : V(C_2H_2) = 1.1 : 1$, GHSV = 120 h^{-1}.

catalyst with an C_2H_2 conversion rate of 92% was reduced. It also showed an easy and efficient regeneration performance.

Furthermore, it is generally believed that Au^{3+} is the active component of catalysts for the C_2H_2 hydrochlorination reaction. The activity recovery of the regenerated catalyst also showed that the reduction and the running off of Au^{3+} were not the main reasons for the catalyst deactivation.

4. Conclusions

Historically, γ-Al_2O_3 was used less as an efficient support to prepare catalysts for C_2H_2 hydrochlorination compared with other carriers. The $AuCl_3$–$CuCl_2$/γ-Al_2O_3 catalyst can attain a 97% conversion rate for C_2H_2 conversion, which was close to that using AC as the support. The results show that using γ-Al_2O_3 as a support gave better mechanical strength and mesoporous (20–50 nm) structure and was thus a potential support for the $AuCl_3$–$CuCl_2$ bimetal catalyst. It was the strong basic sites rather than the textural properties or the acidic sites that determined its unusual activity compared to others. Furthermore, modifying the support with KOH can increase the activity and prolong the life span. The carbon deposition was the main reason for its fast deactivation and the actual amount of coke deposition was 18.0%. Although with a short life span at present, its thermostability and mechanical strength revealed its excellent regeneration ability. Therefore, it is believed that γ-Al_2O_3 has great potential in view of its increased life span and reduced cost. In the meantime, this should be studied further in future research.

Acknowledgements

We are grateful to the Fundamental Research Funds for the Central Universities (no. WA1214003) and the Technology Development Funds for the Tanggu of Binhai New Area, Tianjin, China (no. 2012STHB04-01).

References

1 X. B. Wei, H. B. Shi, W. Z. Qian, G. H. Luo, Y. Jin and F. Wei, *Ind. Eng. Chem. Res.*, 2009, **48**, 128.
2 G. J. Hutchings and D. T. Grady, *Appl. Catal.*, 1985, **17**, 155.
3 N. Pirrone, S. Cinnirella, X. Feng, R. Finkelman, H. R. Friedli, J. Leaner, R. Mason, A. B. Mukherjee, G. B. Stracher, D. G. Streets and K. Telmer, *Atmos. Chem. Phys.*, 2010, **10**, 5951.
4 H. Z. Gu, X. S. Xu, A. A. Chen, A. Ping and X. H. Yan, *Catal. Commun.*, 2013, **41**, 65–69.
5 B. B. Chen, X. B. Zhu, M. Crocker, Y. Wang and C. Shi, *Catal. Commun.*, 2013, **42**, 93.
6 M. Conte, A. F. Carley, C. Heirene, D. J. Willock, P. Johnston, A. A. Herzing, C. J. Kiely and G. J. Hutchings, *J. Catal.*, 2007, **250**, 231.
7 M. Conte, A. F. Carley, G. Attard, A. A. Herzing, C. J. Kiely and G. J. Hutchings, *J. Catal.*, 2008, **257**, 190.
8 S. J. Wang, B. X. Shen and Q. L. Song, *Catal. Lett.*, 2010, **134**, 102.
9 X. B. Wei, F. Wei, W. Z. Qian, G. H. Luo, H. B. Shi and Y. Jin, *Chin. J. Process Eng.*, 2008, **8**, 1218.
10 H. Y. Zhang, B. Dai, X. G. Wang, L. L. Xu and M. Y. Zhu, *J. Ind. Eng. Chem.*, 2012, **18**, 49.
11 J. Zhao, X. Cheng and L. Wang, *et al.*, *J. Catal.*, 2014, **144**, 2191–2197.
12 X. Yang, C. Jiang and Z. Yang, *J. Mater. Sci. Technol.*, 2014, **30**, 434–440.
13 X. G. Cheng, J. G. Zhao, L. Wang, R. F. Ren, H. H. Yang and B. X. Shen, *Chem. Res. Chin. Univ.*, 2014, **3**, 582.
14 H. L. Chih, D. L. Shawn and F. L. Jyh, *Catal. Lett.*, 2003, **89**, 235.
15 J. C. Yeong and T. Y. Chuin, *J. Catal.*, 2001, **200**, 59.
16 L. J. Marta, J. Wojciech, B. Magdalena, K. Zbigniew, K. Leszek and K. Zbigniew, *Top. Catal.*, 2009, **52**, 1037.
17 E. D. Park and J. S. Lee, *J. Catal.*, 1999, **186**, 1–11.
18 J. Zhao, J. Xu and J. Xu, *J. Chem. Eng.*, 2014, **262**, 1152–1160.
19 J. Okal, W. Tylus and L. Kępiński, *J. Catal.*, 2004, **225**, 498–509.
20 E. B. Cornelius, T. H. Milliken, G. A. Mills and A. G. Oblad, *J. Phys. Chem.*, 1955, **59**, 809.
21 S. L. Wang, C. T. Johnston and D. L. Bish, *J. Colloid Interface Sci.*, 2003, **260**, 26–35.